DIGITAL IMAGE PROCESSING

WILLIAM K. PRATT

Professor of Electrical Engineering
Image Processing Institute
University of Southern California
Los Angeles, California

A WILEY–INTERSCIENCE PUBLICATION
JOHN WILEY & SONS
New York / Chichester / Brisbane / Toronto

GOOGLE EXHIBIT 1018

To my son Michael

Copyright © 1978 by John Wiley & Sons, Inc.

All rights reserved. Published simultaneously in Canada.

Reproduction or translation of any part of this work beyond that permitted by Sections 107 or 108 of the 1976 United States Copyright Act without the permission of the copyright owner is unlawful. Requests for permission or further information should be addressed to the Permissions Department, John Wiley & Sons, Inc.

Library of Congress Cataloging in Publication Data

Pratt, William K.
Digital image processing.

"A Wiley-Interscience publication."
Includes bibliographical references and index.
1. Image processing. I. Title.

TA1632.P7 1978 621.3815'42 77-20888
ISBN 0-471-01888-0

Printed in the United States of America

10 9 8 7 6 5 4 3 2

PREFACE

The field of digital image processing has grown considerably during the past decade with the increased utilization of imagery in myriad applications coupled with improvements in the size, speed, and cost effectiveness of digital computers and related signal processing technologies. Image processing has found a significant role in scientific, industrial, biomedical, space, and governmental applications. Such applications include the digital transmission of spacecraft imagery and personal telephone carrier television; the resolution improvement of electron microscope images and the compensation of sensor and transmission errors of pictures transmitted from deep-space probes; the automatic classification of terrain and detection of resources from earth resources satellite pictures; the formation and enhancement of biomedical imagery, including radiographs, thermograms, and nuclear scanned images; automatic map making from aerial photographs; and the detection of cracks and flaws in machine parts from industrial radiographs. In the future image processing will, no doubt, be utilized to a greater extent to aid medical practitioners in the detection and diagnosis of disease from biomedical images. Industrial applications should abound; image processing systems will analyze scenes from the "eyes" of industrial automatons to control their actions. Efficient image coding techniques offer the promise of scores of personal two-way television channels for homes and businesses. The list is limited only by imagination.

This book is intended to serve as a text for an electrical engineering or computer science graduate course in digital image processing, and as a reference for practicing engineers and scientists engaged in image processing research and development activities. Digital image processing is a broad subject encompassing studies of physics, physiology, electrical engineering, computer science, and mathematics. Readers are assumed to have an undergraduate technical background in one of these areas. Knowledge of linear system theory, vector algebra, probability, and random processes is certainly beneficial, but not absolutely necessary.

The book is divided into six parts. Part 1 contains three chapters concerned with the characterization of continuous images. Topics covered include the mathematical representation of continuous images, the psychophysical properties of human vision, and photometry and colorimetry. In Part 2 image sampling and quantization techniques are explored along

images have been photographically recorded by Dr. Clifford Reader of Ford Aerospace and Communications Corp. of Palo Alto, California. The gracious assistance of these individuals is sincerely appreciated and acknowledged.

Finally, words of appreciation for my sponsor, the Information Processing Techniques Office of the Advanced Research Projects Agency. This work was supported in part by ARPA and was monitored by the Air Force Range Measurements Laboratory under Contract No. F-08606-72-C-0008 and by the Wright-Patterson Air Force Base under Contract No. F-33615-76-C-1203.

W.K.P.

CONTENTS

Part 1. Continuous Image Characterization

1. Mathematical Characterization of Continuous Images 3
2. Psychophysical Properties of Vision 25
3. Photometry and Colorimetry 50

Part 2. Digital Image Characterization

4. Image Sampling and Reconstruction 93
5. Mathematical Characterization of Discrete Images 121
6. Image Quantization 140
7. Sampled Image Quality Measures 162

Part 3. Discrete Two-Dimensional Linear Processing

8. Linear Operators 201
9. Superposition Operator 214
10. Two-Dimensional Unitary Transforms 232
11. Two-Dimensional Linear Processing Techniques 279

Part 4. Image Enhancement and Restoration

12. Image Enhancement 307
13. Image Restoration Models 345
14. Algebraic Spatial Image Restoration Techniques 378
15. Specialized Spatial Image Restoration Techniques 426
16. Luminance, Color, and Spectral Image Restoration 447

Part 5. Image Analysis

17. Image Feature Extraction 471
18. Symbolic Image Description 514
19. Image Detection and Registration 551
20. Image Understanding Systems 568

Part 6. Image Coding

21. Analog Processing Image Coding 591
22. Digital Point Processing Image Coding 616
23. Digital Spatial Processing Image Coding 662
24. Image Coding Performance Analysis 710

Appendix

1. Selected References 733
2. Color Coordinate Conversion 736
3. Statistical Source Coding 741

Index 743

DIGITAL IMAGE PROCESSING

TABLE 12.2-1. Histogram modification transfer functions

Output Probability Density Model		Transfer Function[a]
Uniform	$p_g(g) = \dfrac{1}{g_{max} - g_{min}} \quad g_{min} \le g \le g_{max}$	$g = [g_{max} - g_{min}]P_f(f) + g_{min}$
Exponential	$p_g(g) = \alpha \exp\{-\alpha(g - g_{min})\} \quad g \ge g_{min}$	$g = g_{min} - \dfrac{1}{\alpha}\ln[1 - P_f(f)]$
Rayleigh	$p_g(g) = \dfrac{g - g_{min}}{\alpha^2}\exp\left\{-\dfrac{(g - g_{min})^2}{2\alpha^2}\right\} \quad g \ge g_{min}$	$g = g_{min} + \left[2\alpha^2 \ln\left(\dfrac{1}{1 - P_f(f)}\right)\right]^{1/2}$
Hyperbolic (Cube Root)	$p_g(g) = \dfrac{1}{3}\dfrac{g^{-2/3}}{g_{max}^{1/3} - g_{min}^{1/3}}$	$g = ([g_{max}^{1/3} - g_{min}^{1/3}][P_f(f)] + g_{min}^{1/3})^3$
Hyperbolic (Logarithmic)	$p_g(g) = \dfrac{1}{g[\ln(g_{max}) - \ln(g_{min})]}$	$g = g_{min}\left[\dfrac{g_{max}}{g_{min}}\right]^{P_f(f)}$

[a] The cumulative probability distribution, $P_f(f)$, of the input image is approximated by its cumulative histogram

$$P_f(f) \approx \sum_{m=0}^{f} H_F(m)$$

12.3. NOISE CLEANING

An image may be subject to noise and interference from several sources including electrical sensor noise, photographic grain noise, and channel errors. These noise effects can be minimized by classical statistical filtering techniques to be discussed in Chapter 14. Another approach is the application of spatial ad hoc processing techniques.

Image noise arising from a noisy sensor or channel transmission errors usually appears as discrete isolated pixel variations that are not spatially correlated. Pixels that are in error often appear markedly different from their neighbors. This observation is the basis of many noise-cleaning algorithms (8–11). Figure 12.3-1 describes a simple "out-range" noise-cleaning method. With this technique, each pixel is sequentially examined, and if the magnitude of a pixel is greater than the average brightness of its immediate neighbors by some threshold level, it is replaced by the average value. Figure 12.3-2 provides examples of this noise-cleaning algorithm for PCM pictures subjected to simulated binary symmetric channel errors with an error rate of 10^{-2}.

Noise in an image generally has a higher spatial frequency spectrum than the normal image components because of its spatial decorrelatedness. Hence simple low-pass spatial filtering can be effective for noise smoothing. Following the techniques outlined in Part 3, an output $M \times M$ image array Q is formed by discrete convolution of the input $N \times N$ image array F with the $L \times L$ convolution array H according to the relation

$$Q(m_1, m_2) = \sum_{n_1}\sum_{n_2} F(n_1, n_2)H(m_1 - n_1 + 1, m_2 - n_2 + 1) \qquad (12.3\text{-}1)$$

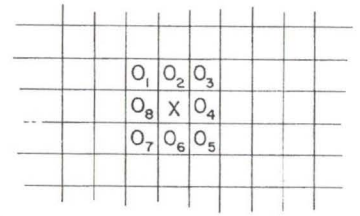

IF $\left[X - \frac{1}{8}\sum_{i=1}^{8} O_i\right] > \epsilon$ THEN

$X = \frac{1}{8}\sum_{i=1}^{8} O_i$

FIGURE 12.3-1. Example of noise-cleaning algorithm.

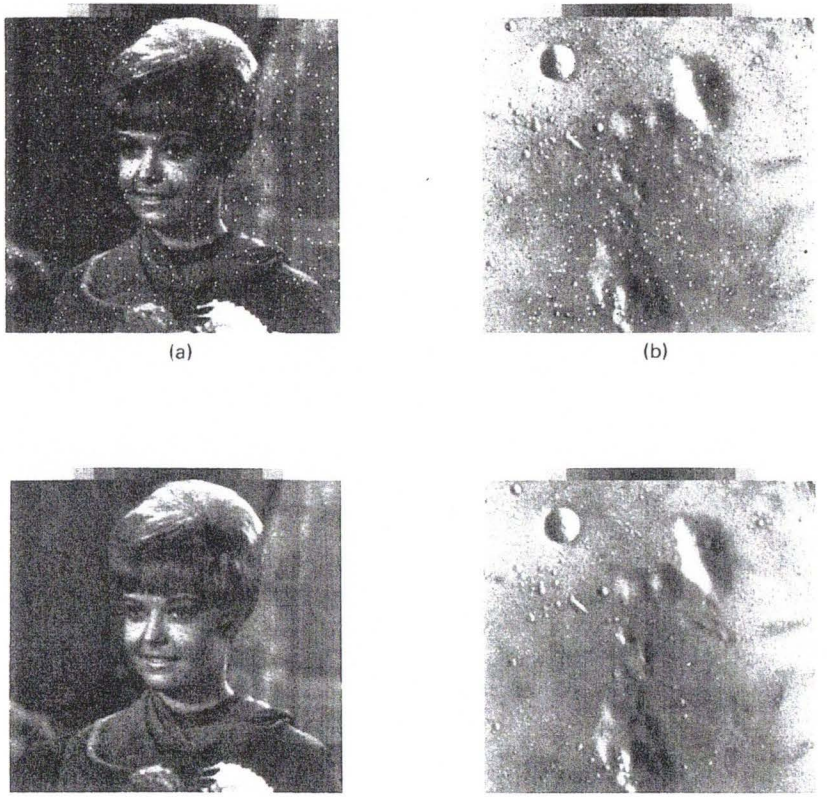

(a) (b) (c) (d)

FIGURE 12.3-2. Examples of noise cleaning with out-range algorithm with $\varepsilon = 49$. (a) Noisy GIRL. (b) Noisy MOON. (c) Cleaned GIRL. (d) Cleaned MOON.

For noise smoothing H should be of low-pass form with all positive components. Several convolution arrays of low-pass form are listed below.

Mask 1

$$\mathbf{H} = \frac{1}{9}\begin{bmatrix} 1 & 1 & 1 \\ 1 & 1 & 1 \\ 1 & 1 & 1 \end{bmatrix} \tag{12.3-2a}$$

Mask 2

$$\mathbf{H} = \frac{1}{10}\begin{bmatrix} 1 & 1 & 1 \\ 1 & 2 & 1 \\ 1 & 1 & 1 \end{bmatrix} \tag{12.3-2b}$$

Mask 3

$$\mathbf{H} = \frac{1}{16}\begin{bmatrix} 1 & 2 & 1 \\ 2 & 4 & 2 \\ 1 & 2 & 1 \end{bmatrix} \tag{12.3-2c}$$

These arrays, which are often called noise-cleaning masks, are normalized to unit weighting so that the noise-cleaning process does not introduce a brightness bias in the processed image. The effect of noise cleaning with these arrays is shown in Figure 12.3-3. If the required noise mask becomes large in order to achieve adequate noise cleaning, it is usually more computationally efficient to perform the convolution operation indirectly by the Fourier filtering techniques outlined in Chapter 11.

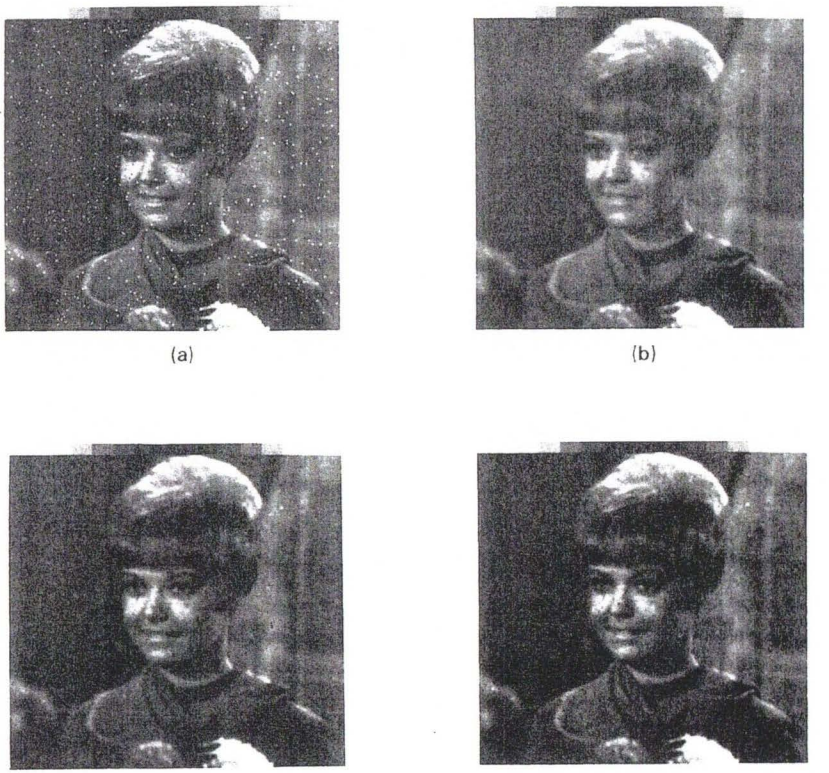

(a) (b) (c) (d)

FIGURE 12.3-3. Examples of noise cleaning with low-pass convolution masks. (a) Noisy original. (b) With mask No. 1. (c) With mask No. 2. (d) With mask No. 3.

12.4. EDGE CRISPENING

Psychophysical experiments indicate that a photograph or visual signal with accentuated edges is often more subjectively pleasing than an exact photometric reproduction. Edge enhancement or crispening can be accomplished in a variety of ways.

For electronically scanned images the scanner signal can be passed through an electrical filter with a high-frequency bandpass characteristic. Another possibility for scanned images is the technique of unsharp masking (12). In this process the image is effectively scanned by two overlapping apertures, one at normal resolution and the other at a lower resolution, producing normal and low-resolution images $F(j,k)$ and $F_L(j,k)$, respectively. A masked image

$$F_M(j,k) = cF(j,k) - (1-c)F_L(j,k) \tag{12.4-1}$$

is then formed electronically where c is a proportionality constant. Typically, c is in the range of $\frac{3}{5}$ to $\frac{5}{6}$ so that the ratio of normal to low-resolution components in the masked image is from 1.5:1 to 5:1. Figure 12.4-1 illustrates typical scan signals for scanning over a sharp edge. The masked signal has a longer duration edge gradient as well as an overshoot compared to the original high-resolution signal. Subjectively, the apparent sharpness of the image is improved.

Edge crispening can also be accomplished by discrete convolutional filtering, as defined by Eq. 12.3-1, in which the impulse response array H is

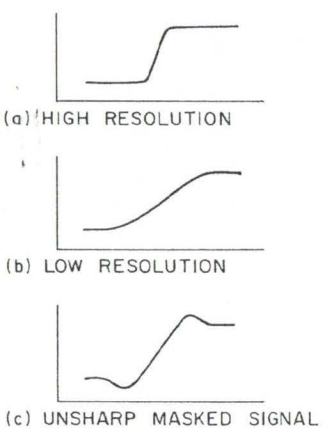

FIGURE 12.4-1. Waveforms in an unsharp masking image enhancement system.

of high-pass form (13–15). Several typical high-pass masks are listed below.

Mask 1

$$\mathbf{H} = \begin{bmatrix} 0 & -1 & 0 \\ -1 & 5 & -1 \\ 0 & -1 & 0 \end{bmatrix} \tag{12.4-2}$$

Mask 2

$$\mathbf{H} = \begin{bmatrix} -1 & -1 & -1 \\ -1 & 9 & -1 \\ -1 & -1 & -1 \end{bmatrix} \tag{12.4-3}$$

Mask 3

$$\mathbf{H} = \begin{bmatrix} 1 & -2 & 1 \\ -2 & 5 & -2 \\ 1 & -2 & 1 \end{bmatrix} \tag{12.4-4}$$

These masks possess the property that the sum of their elements is unity. Figure 12.4-2 provides examples of edge crispening with unsharp masking and with high-pass masks.

Another form of edge enhancement called statistical differencing (7, 16, p. 100) involves the generation of an image by dividing each pixel value by its measured statistical standard deviation $\sigma(j,k)$ according to the relation

$$G(j,k) = \frac{F(j,k)}{\sigma(j,k)} \tag{12.4-5}$$

where the standard deviation

$$\sigma^2(j,k) = \underbrace{\sum_j \sum_k}_{j,k \in N(j,k)} [F(j,k) - \bar{F}(j,k)]^2 \tag{12.4-6}$$

is computed over some neighborhood $N(j,k)$ of the pixel at coordinate (j,k). The function $\bar{F}(j,k)$ is the mean value of the original image at point (j,k), which is approximated by blurring or smoothing the original image by a smoothing operator of low-pass form as described by Eq. 12.3-1. The enhanced image $G(j,k)$ will be increased in amplitude with respect to the original image $F(j,k)$ at edge points that deviate from their neighbors, and decreased in relative amplitude elsewhere. It should be stressed that noise components may be accentuated as well as valid edge structure.

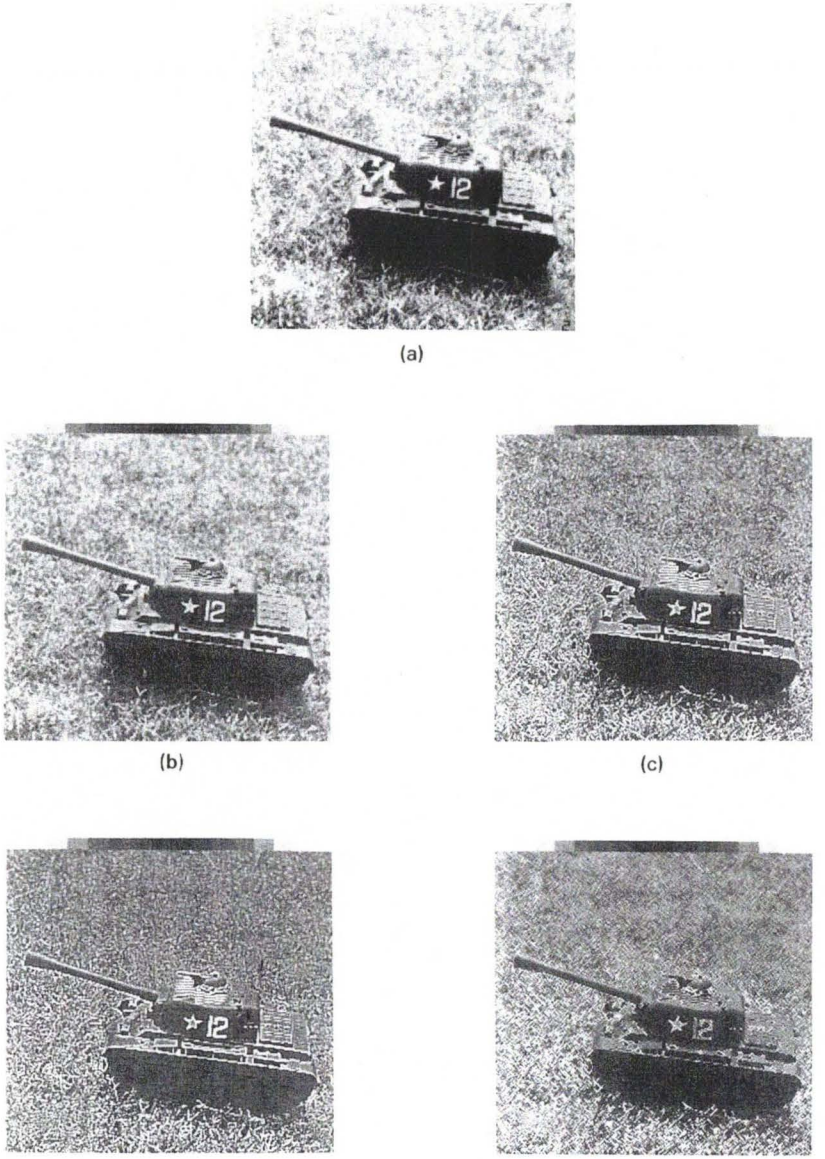

FIGURE 12.4-2. Examples of edge crispening with unsharp masking and with high pass masks. (a) Original. (b) Unsharp masking $c = \frac{3}{4}$. (c) Mask No. 1. (d) Mask No. 2. (e) Mask No. 3.

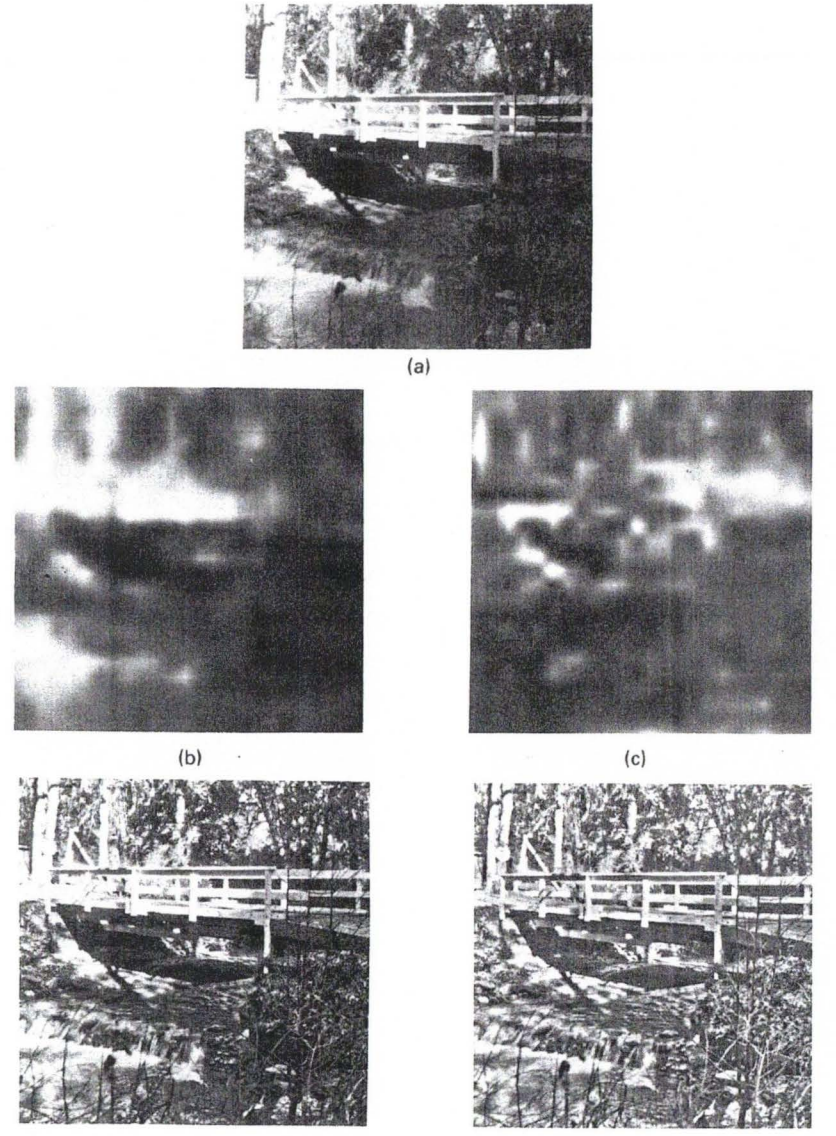

FIGURE 12.4-3. Example of statistical differencing (17). Photographs provided by R. H. Wallis, Stanford Technology Corp., Sunnyvale, California. (a) Original. (b) Neighborhood average. (c) Neighborhood standard deviation. (d) Enhancement $\alpha = 0.8$, $m_d = 128$, $\alpha_d = 85$, $A = 6$. (e) Enhancement $\alpha = 0.1$, $m_d = 128$, $\alpha_d = 85$, $A = 6$.

Wallis (17) has suggested a generalization of the statistical differencing operator in which the enhanced image is forced to a form with desired first- and second-order moments. The operator is defined by

$$G(j,k)=[F(j,k)-\bar{F}(j,k)]\left[\frac{A\sigma_d}{A\sigma(j,k)+\sigma_d}\right]+[\alpha m_d+(1-\alpha)\bar{F}(j,k)] \tag{12.4-7}$$

where m_d and σ_d represent desired mean and standard deviation factors, A is a gain factor that prevents overly large output values when $\sigma(j,k)$ is small, and α is a proportionality factor controlling the ratio of edge to background composition of the enhanced image. Figure 12.4-3 illustrates the effect of statistical differencing on a scene with deep sun shadows. In this example the experimental mean and standard deviation factors are computed in nonoverlapping 20×20 pixel blocks. Bilinear interpolation of the four nearest block values is used to compute the mean and standard deviation at each point.

12.5. TRANSFORM PROCESSING

Unitary image transforms such as the Fourier and Hadamard transforms provide a spectral decomposition of an image into coefficients that tend to isolate certain features of an image. For example, the first or d.c. spectral component is proportional to the average image brightness, and the higher spatial frequency or sequency components are measures of the image edge content. This inherent property of many image transforms can be exploited for image enhancement. Let $\mathcal{F}(u,v)$ represent the discrete two-dimensional unitary transform of a sampled image $F(j,k)$ as given by the transform pairs

$$\mathcal{F}(u,v)=\sum_{j=0}^{N-1}\sum_{k=0}^{N-1}F(j,k)A(j,k;u,v) \tag{12.5-1a}$$

$$F(j,k)=\sum_{u=0}^{N-1}\sum_{v=0}^{N-1}\mathcal{F}(u,v)B(j,k;u,v) \tag{12.5-1b}$$

where $A(j,k;u,v)$ and $B(j,k;u,v)$ are the forward and inverse transform kernels, respectively.

Coefficient Rooting (3)

In the coefficient rooting process the magnitude of each transform domain coefficient is raised to a power and the sign or phase portion of the

coefficient is retained. The modified transform coefficient is given by

$$\tilde{\mathcal{F}}(u,v)=\frac{\mathcal{F}(u,v)}{|\mathcal{F}(u,v)|}|\mathcal{F}(u,v)|^{\alpha}=\mathcal{F}(u,v)|\mathcal{F}(u,v)|^{\alpha-1} \tag{12.5-2}$$

For a Fourier transform in which

$$\mathcal{F}(u,v)=\mathcal{M}(u,v)\exp\{i\Phi(u,v)\} \tag{12.5-3}$$

where $\mathcal{M}(u,v)$ and $\Phi(u,v)$ are the magnitude and phase components of the transform coefficient, respectively, the modified coefficient becomes

$$\tilde{\mathcal{F}}(u,v)=[\mathcal{M}(u,v)]^{\alpha}\exp\{i\Phi(u,v)\} \tag{12.5-4}$$

In the limiting case for which $\alpha=0$, the modified transform coefficient is simply the phase component of the image. If the rooting factor α is chosen to be less than unity, the coefficient rooting operation tends to reduce the magnitude of high-amplitude transform coefficients and increase the amplitude of low-magnitude coefficients. The result of this energy redistribution in the transform domain is often a better utilization of the image dynamic range, and a more subjectively pleasing reproduction. Figure 12.5-1 contains examples of the coefficient rooting process.

Generalized Cepstrum

Another method of nonlinear transform image enhancement consists of taking the logarithm of each transform coefficient. Qualitatively, this operation tends to reduce the dynamic range of samples in the transform domain and increase the dynamic range in the image domain upon reconstruction. Bogert, Healy, and Tukey (18) have introduced a similar transformation for speech processing as a means of detecting echoes. In their transformation, called the cepstrum,* the power spectrum is taken of the logarithm of the power spectrum of a signal. This concept has been extended by Oppenheim, Schafer, and Stockham (19), who defined the complex cepstrum as the Fourier transform of the logarithm of the Fourier transform. For an arbitrary transform a generalized logarithmic transform cepstrum is defined as (20)

$$\tilde{F}(j,k)=K\sum_{u=0}^{N-1}\sum_{v=0}^{N-1}[\ln\{a+b|\mathcal{F}(u,v)|\}]\frac{\mathcal{F}(u,v)}{|\mathcal{F}(u,v)|}B(j,k;u,v) \tag{12.5-5}$$

* Cepstrum is a juxtaposition of letters of the word Spectrum.